

# Geochemistry and geochronology of Early Mesozoic tholeiites from Central Morocco

By L. FIECHTNER, H. FRIEDRICHSEN and K. HAMMERSCHMIDT, Berlin\*)

With 14 figures and 5 tables

## Zusammenfassung

Aus Zentralmarokko (Zentraler Hoher Atlas, Mittlerer Atlas, Haute Moulouya) wurden, in kontinentale Rotserien des frühen Mesozoikums (Trias-Lias) eingeschaltete Tholeiite geochemisch und geochronologisch untersucht. Haupt-, Spuren- und Seltene Erden-Elementgehalte klassifizieren die Vulkanite als basaltische bis andesitisch-basaltische, quarznormative Tholeiite. Einige Spurenelementverhältnisse (Zr/Nb, Zr/Y, Y/Nb, Ti/V) weisen auf eine MORB-ähnliche (P- bis N-typisch) Zusammensetzung hin. Die erhöhten LILE-Gehalte, die negative Nb-Anomalie und die  $^{87}\text{Sr}/^{86}\text{Sr}$ -Anfangsverhältnisse (0.7064–0.7069) zeigen eine krustale Komponente an (13–17 Gew%). Unterschiedliche  $^{87}\text{Sr}/^{86}\text{Sr}$ -Verhältnisse karbonatischer Mineralseparate aus verschiedenen Lavaströmen weisen auf mehrere Alterationszyklen hin, deren Alterationslösungen keine Meerwasserzusammensetzung besaßen.  $^{40}\text{Ar}/^{39}\text{Ar}$ -Datierungen an Plagioklassen ergaben Extrusionsalter zwischen  $210.4 \pm 2.1$  Ma und  $196.3 \pm 1.2$  Ma. Stratigraphisch umfaßt dies den Zeitraum zwischen Nor (Rhät?) und oberem Sinemur.

## Abstract

From Central Morocco (Central High Atlas, Middle Atlas, Haute Moulouya) continental tholeiites were investigated geochemically and geochronologically. These tholeiites are intercalated within continental redbeds of the Early Mesozoic

(Triassic-Liassic). The major, trace and rare earth element contents classify these volcanic rocks as basaltic to andesitic-basaltic, quartz-normative tholeiites. Some trace element ratios (e.g. Zr/Nb, Zr/Y, Y/Nb, Ti/V) suffer a heterogeneous source with a composition similar to MORB (P- to N-type). The enriched LILE contents, the negative Nb anomaly and the initial  $^{87}\text{Sr}/^{86}\text{Sr}$  ratios (0.7064–0.7069) reveal the presence of a crustal component up to 13–17 wt%.  $^{87}\text{Sr}/^{86}\text{Sr}$  ratios of carbonate mineral separates from different lava flows show different cycles of alteration; however, the major and trace element chemistry together with Sr isotope evidence, indicate that the alteration phases are not submarine in origin.  $^{40}\text{Ar}/^{39}\text{Ar}$  age determinations on translucent plagioclase phenocrysts yield extrusion ages which range between  $210.4 \pm 2.1$  Ma and  $196.3 \pm 1.2$  Ma. These ages correspond to a stratigraphic period between the Norian (Rhaetian?) and the Upper Sinemurian.

## Résumé

Des tholéiites du Maroc central (Haut Atlas central, Moyen Atlas, Haute Moulouya) ont fait l'objet d'une investigation géochimique et géochronologique. Ces tholéiites sont intercalées dans des couches rouges continentales d'âge mésozoïque inférieur (Trias-Lias). Les teneurs en éléments majeurs, en éléments en trace et en terres rares classent ces roches volcaniques comme tholéiites basaltiques à andésito-basaltiques, à quartz normatif. Certains rapports d'éléments en traces (p.

\*) Authors' address: L. FIECHTNER, H. FRIEDRICHSEN and K. HAMMERSCHMIDT, Institut für Mineralogie, FR Geochemie, Boltzmannstr. 18–20, W–1000 Berlin 33, FRG.

ex.: Zr/Nb, Zr/Y, Y/Nb, Ti/V) indiquent une composition analogue au MORB (type P à N). La teneur élevée en LILE, l'anomalie négative du Nb et les rapports initiaux  $^{87}\text{Sr}/^{86}\text{Sr}$  (0,7064 à 0,7069) révèlent la présence d'un composant crustal dans la proportion de 13 à 17% en poids. Les rapports  $^{87}\text{Sr}/^{86}\text{Sr}$  de minéraux carbonatés séparés de diverses coulées de lave montrent l'existence de plusieurs cycles d'altération; toutefois, le chimisme des majeurs et des traces, ainsi que les données isotopiques du Sr, indiquent que ces phases d'altération ne sont pas sous-marines. Les mesures d'âge par  $^{40}\text{Ar}/^{39}\text{Ar}$  effectuées sur des plagioclases fournissent des âges d'extrusion compris entre  $210,4 \pm 2,1$  Ma et  $196,3 \pm 1,2$  Ma. Ces âges correspondent à une période située entre le Norien (Rhétien?) et le Sinémurien supérieur.

### Краткое содержание

Провели геохимические и геохронологические исследования толеитов, включенных в материковые красноцветные свиты раннего мезозоя триас-лейас из центрального Марокко. На основании распределения главных и микроэлементов, а также Редких Земель считают, что эти вулканы можно отнести к базальтовым до андезитно-базальтовым толеитам с нормальным содержанием кварца. На основании соотношения микроэлементов Zr/Nb, Zr/Y, Y/Nb, Ti/V предполагают состав, подобный MORB типа P до N. Повышенное содержание LILE, отрицательная аномалия Nb и исходные соотношения изотопов стронция  $^{87}\text{Sr}/^{86}\text{Sr} = 0,7064-0,7069$  указывают на присутствие компонентов коры в них (13–17 вес.-%).

Различия в соотношениях содержания стронция в карботных минералах из различных потоков лав говорят о многократных циклических изменениях, происходивших в эти промежутки времени, причем содержание элементов во внесенных растворах не соответствовали составу морской воды. Определение возраста по изотопам аргона на плагиоклазах указывают на то, что возраст экструзий составляет  $210,4 \pm 2,1$  Ma –  $196,3 \pm 1,2$  Ma. Стратиграфически этот возраст соответствует норийскому ярусу (рэтскому ?) и верхнему синемюрскому ярусу.

### Introduction

The early Mesozoic evolution of the Atlas system is characterised by repeated volcanic activity.

This volcanism is related to the initial opening of the Atlantic Ocean and the Atlas rift system (MATTAUER et al. (1977), MANN SPEIZER et al. (1978), STETS & WURSTER (1981), JACOB SHAGEN et al. (1988)). K–Ar dating on these volcanic rocks yield extrusion ages which vary from 200 to 180 Ma (MANN SPEIZER et al., 1978). This variation would correspond to a period between the Lower Sinemurian and the Upper Toarcian (ODIN et al., 1982; COWIE & BASSETT, 1989). However, these ages contrast with the stratigraphic position of the volcanic rocks which lie between continental Carnian (COUSMINER & MANN SPEIZER, 1976) and marine Sinemurian (WARME, 1988; HAUPTMANN, 1990). Therefore, the first aim of this work is to determine the extrusion ages on clear plagioclase phenocrysts from these continental tholeiites, using the  $^{40}\text{Ar}/^{39}\text{Ar}$  dating method. The dating problem is compounded by the fact that most of the published geochemical data are limited to major element chemistry, and thus allows only approximate interpretations of the origin and by inference of the timing of these continental tholeiites. Our second aim, therefore, is to search for geochemical and isotopic indications of the magma genesis of these volcanic rocks.

### Geological settings

In the Atlas system the early Mesozoic volcanic rocks are commonly intercalated with Triassic-Liassic redbeds which were deposited in elongated, NE–SW striking basins (LORENZ, 1988), consisting of red fluviatile and alluvial fan type conglomerates, sandstones, lagoon mudstones, and occasionally gypsum and halites. The volcanic rocks are either intercalated in the upper part of the redbeds (pelitic facies) or overlie the redbeds, and are themselves overlain by dolomites of the Imouzzer formation. Occasionally, the volcanic rocks lie discordantly on Paleozoic basement (granites, schists) rocks. The thickness of the redbeds reach up to 1000 m (MATTIS, 1977), while the volcanics vary between 150 and 200 m (SALVAN, 1974). The volcanic sequence consists of one to several lava flows (up to 14 flows, VAN HOUTEN, 1977) sometimes intercalated with mudstones and limestones with lacustric stromatolites and gymnosperm pollen. The fossils within the limestones document a non-marine extrusion environment for the volcanic rocks, whereas the evaporites of the pelitic sequence would point to lagoonal conditions.

## Sample location

The surface and drill sampling points are located in the central High Atlas, the southern Middle Atlas, and the southwest of the Haute Moulouya and are distributed over 11 sampling areas (Fig. 1). The coordinates of the samples are given in terms of the UTM-Grid (Lambert-coordinates). The volcanic series of the drillcore HM 2

(area 8, Fig. 1) consists of nine lava flows (Fig. 2) and the samples were taken at intervals of 0.5–1.0 m.

## Petrography

The volcanic rocks show common textural features and modal compositions which are typical for tholeiites. Primary minerals are plagioclase (An

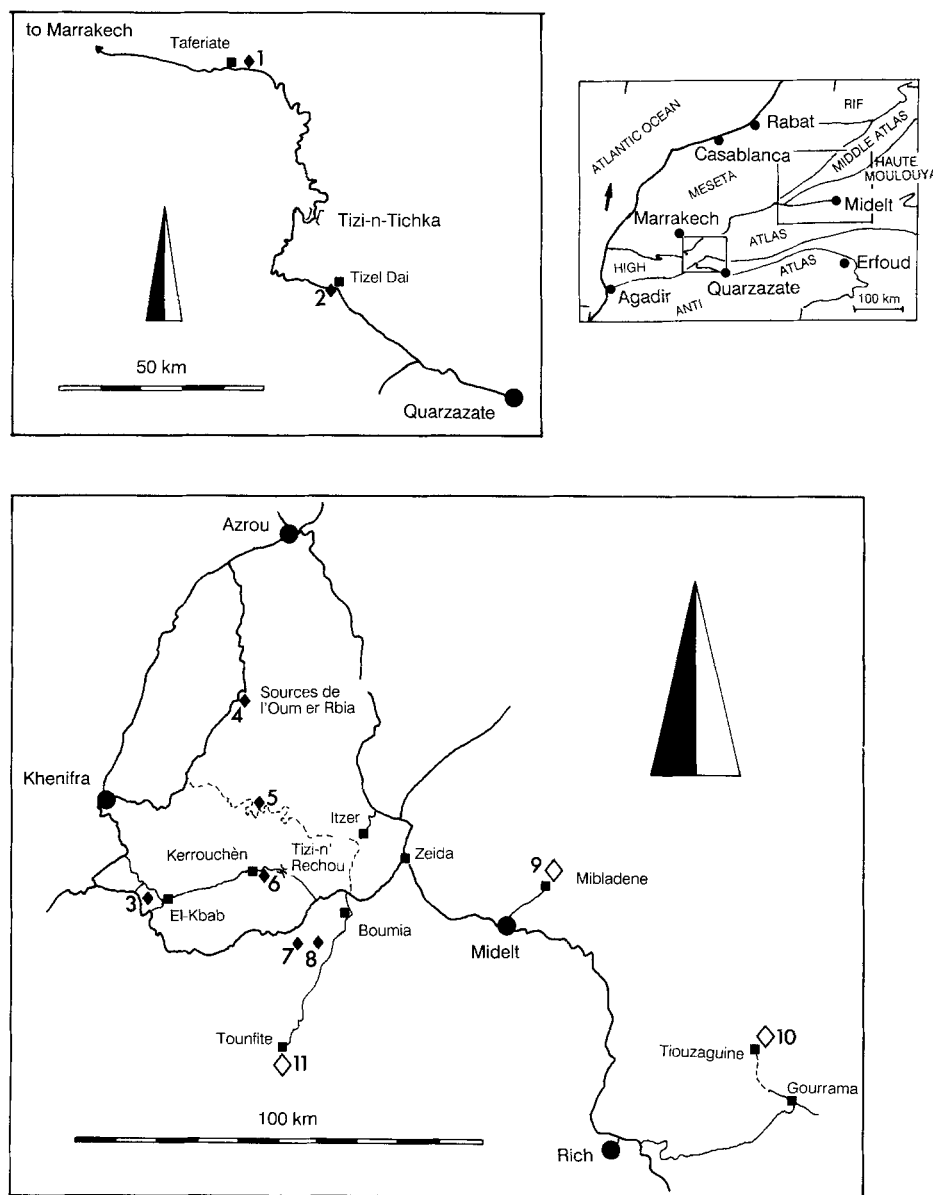


**Fig. 1.** Sketch maps shows the sampling localities (1–7 and 9–11) and the drilling well (8). The filled diamonds indicate samples with age determinations, open diamonds those without age determinations. The exact sampling localities are the following one (UTM-grid):

- 1=Fi 7/88 UTM: 107000/298000; 2=Fi 5/88 UTM: 61100/315700;  
 3=Fi 74/88 UTM: 238600/483500; 4=Fi 111/88 UTM: 272800/498500  
 5=Fi 113/88 UTM: 256500/510000; 6=Fi 1/88 UTM: 244500/505750  
 7=Fi 78/88 UTM: 231900/517000; 8=Fi 16/88 64/88 UTM: 226700/521500

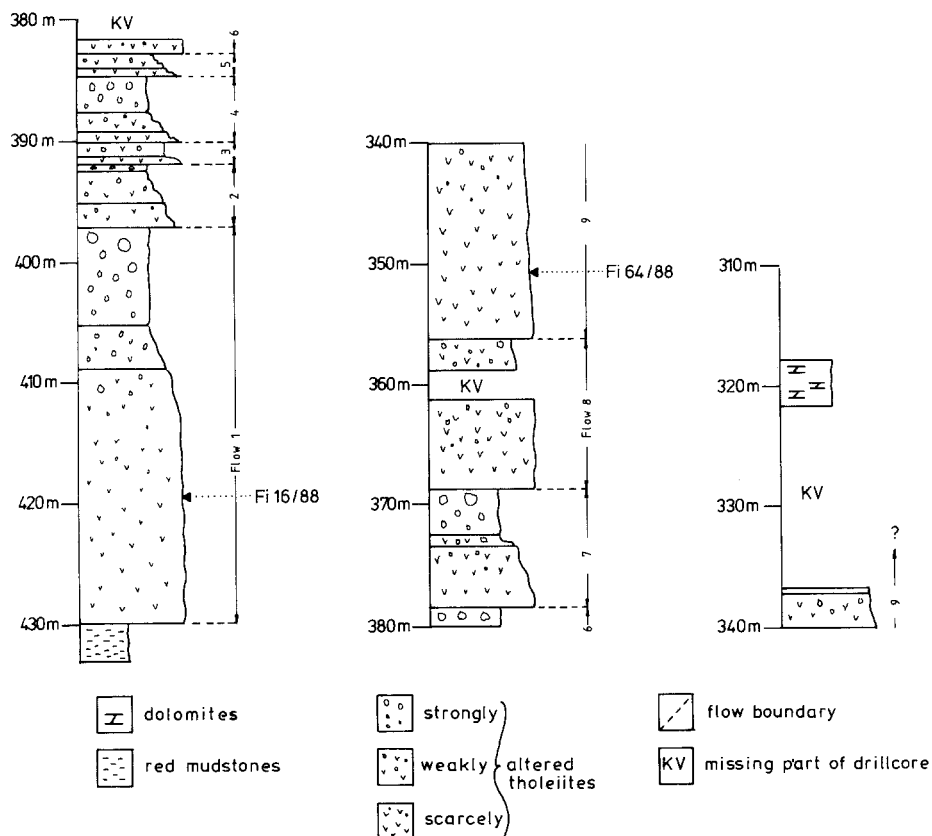


**Fig. 2.** Lithological profile of the volcanic series of drill core HM 2 indicating the stratigraphic position of the samples Fi 16/88 and Fi 64/88 used for geochronological work.

45–68) with albite twinning, pigeonite and Ca-poor augite and Fe-Ti-oxides. The fabrics of the volcanic rocks are dominated by agglomerophiric/porphyric to intergranular/hyalophitic structures. The size of minerals range between 1.2 mm (phenocryst) and 0.1 mm (groundmass). The intergranular/hyalophitic samples can be compared with the intergranular dolerites (group II) of BERTRAND et al. (1982).

Most of the samples are strongly affected by alteration, and have secondary minerals like pumpellyite, saponite, chlorite, carbonate, quartz, zeolite and epidote. These secondary minerals occur in amygdales (1 mm – 2 cm) and joint fillings. The alteration phases of primary plagioclase are either tiny white micas (serizite) or epidotes (saussuritisation). Pyroxenes show signs of saponitization.

#### Analytical methods

A total of 74 volcanics (50 samples from HM 2) were analysed for major and trace elements by XRF, using fused glass disks. In addition, thirty-

nine of these samples were selected for rare earth element (REE) analyses by ICP-EM spectrometry (CNRS; Vandoeuvre Cedex, France).

Rb and Sr isotope ratios of 26 whole rocks, eight pumpellyite-chlorite mixtures and seven carbonate mineral separates (all samples from HM 2) were measured on a thermal ionization mass spectrometer (Finnigan MAT 261). During this investigation the  $^{87}\text{Sr}/^{86}\text{Sr}$  ratio of the standard NBS 987 was measured as  $0.710266 \pm 31$  ( $n=14$ ) normalised to a  $^{86}\text{Sr}/^{88}\text{Sr} = 0.1194$ . All isotope errors are quoted as  $2\sigma$  of the mean, and the  $^{87}\text{Rb}$  decay constant used is  $1.42 \cdot 10^{-11} \text{ a}^{-1}$  (STEIGER & JÄGER, 1977).

$^{40}\text{Ar}/^{39}\text{Ar}$  ages were obtained from nine hand-picked translucent plagioclase separates (> 99% pure). Weighed samples (Tab. 4) and LP-6 standards were irradiated using the facilities at the Kernforschungszentrum Geesthacht (FRG). The inhomogeneity of the neutron fluence was monitored by Ni disks. The data reduction procedure has been described previously (HAMMERSCHMIDT, 1986). The J-value was determined as  $0.02129 \pm 67$  ( $1\sigma$ ) using biotite LP-6 (Ingamells & Engels, 1977)

as an age standard. The Ar isotope composition were determined by a dedicated Ar mass spectrometer. The reciprocal sensitivity is determined as  $(5.6 \pm 0.2) * 10^{-10} \text{ cm}^3 \text{ STP/mV}$  using a known volume of an Ar standard. The mass discrimination per amu amounts to  $6.3 * 10^{-3} (\pm 0.2\%)$ . In the temperature range of between  $350^\circ$  and  $1200^\circ\text{C}$  the blank of  $^{40}\text{Ar}$  never exceeds  $(2.0 \pm 0.2) * 10^{-9} \text{ cm}^3 \text{ STP}$  with a  $^{40}\text{Ar}/^{36}\text{Ar}$  ratio of  $285 \pm 25$ . The blank values for the other Ar isotopes are at least two orders of magnitude lower. For the decay constants and the isotope ratios the recommended values of STEIGER & JÄGER (1977) are used.

## Geochemistry

### Results and discussion

The geochemistry of the studied volcanic rocks reveals a uniform compositional range. Systematic trends in the volcanic sequence are only apparent in the drill core between flow 1 and 9. Tab. 1 gives the mean values of the element concentrations for the fresh samples.

### Major elements

The studied rocks can be classified as basaltic to andesitic-basaltic, quartz-normative tholeiites (DE LA ROCHE et al., 1982). According to KUNO (1950) the rock data plot in the field of pigeonitic basaltic rock and in the AFM-diagram (McDONALD & KATSURA, 1964) the rocks occupy the tholeiitic basalt field. The [Mg]-value ( $\text{Mg}/\text{Mg} + \text{Fe}^{2+}$  atomic ratio with an assumed  $\text{Fe}^{3+}/\text{Fe}^{2+}$  ratio of 0.15) is  $0.68 \pm 5 (1\sigma)$  and indicate the primitive character of these continental tholeiites (CT) compared to other CT (DUPUY & DOSTAL, 1984). The constant [Mg]-values suggest that the rocks have not suffered extensive crystal fractionation. In the  $\text{FeO}/\text{Al}_2\text{O}_3/\text{MgO}$  diagram of PEARCE et al. (1977) most of the samples plot in the field of »ocean ridge and floor« basalts, which is typical for Triassic-Jurassic continental tholeiites, and indicate the similarity of these early Mesozoic CTs to MORB. The calculated  $\text{TiO}_2/\text{P}_2\text{O}_5$  ratios varying between 7 and 11 are similar to those of T- and P-type MORBs (8–11, after SUN et al., 1979). The different  $\text{TiO}_2$  contents of flow 1 and 9 (HM 2) suggest various degrees of partial melting. After a model according to SUN and NESBITT (1977) assuming a Ti content of 0.125 wt% in the source the cal-

culated degree of melting are 16% (flow 1) and 22% (flow 9). Using  $\text{Al}_2\text{O}_3/\text{TiO}_2$  and  $\text{CaO}/\text{TiO}_2$  ratios the composition of the mode of the residuum can be estimated (SUN et al., 1979), which consists here of plagioclase, pyroxene, olivine  $\pm$  spinel. Because the  $\text{Al}_2\text{O}_3/\text{TiO}_2$  and  $\text{CaO}/\text{TiO}_2$  ratios in flow 1 are lower than in flow 9, the resulting modal contents of plagioclase and pyroxene in the residuum for flow 1 are higher than in flow 9. The estimated mineral assemblage of the residuum suggest a low pressure fractionation. This statement is supported by the model of THOMPSON

	HM 2 (flow 1)		HM 2 (flow 9)	
	n=9	$\sigma$	n=9	$\sigma$
$\text{SiO}_2$ (wt%)	51.54	0.41	51.62	1.01
$\text{TiO}_2$	1.37	0.06	1.10	0.03
$\text{Al}_2\text{O}_3$	13.80	0.29	13.77	0.59
$\text{Fe}_2\text{O}_3$	10.19	0.85	11.17	1.92
MnO	0.12	0.02	0.11	0.03
MgO	9.22	0.82	8.14	0.69
CaO	8.30	0.49	9.59	0.74
$\text{Na}_2\text{O}$	1.92	0.28	1.78	0.27
$\text{K}_2\text{O}$	0.92	0.14	0.73	0.09
$\text{P}_2\text{O}_5$	0.16	0.02	0.13	0.02
L.O.I.	1.93	0.44	1.43	0.54
total	99.71	0.68	99.72	0.32
[Mg]-value	0.673	0.080	0.624	0.090
Ba (ppm)	232	25	168	17
Cr	411	29	297	22
Nb	13	1	6	1
Ni	136	13	135	34
Rb	25	8	26	3
Sr	265	13	195	15
V	280	9	268	11
Y	22	2	21	2
Zn	150	125	78	14
Zr	140	13	103	5
La	15	2	10	1
Ce	38	5	26	2
Nd	18	2	12	1
Sm	4.7	0.5	3.3	0.4
Eu	1.3	0.1	0.9	0.1
Gd	4.5	0.3	3.5	0.3
Dy	4.3	0.4	3.6	0.3
Er	2.3	0.2	2.0	0.2
Yb	2.0	0.2	1.8	0.2
Lu	0.34	0.03	0.34	0.04
$(\text{La}/\text{Yb})_N$	5.1	0.8	3.6	0.5
$\text{Eu}^*$	0.86	0.08	0.81	0.08
$(^{87}\text{Sr}/^{86}\text{Sr})_0$	$0.706704 \pm 25$		$0.706577 \pm 13$	

Table 1. Mean values (n=9) with standard deviation ( $\sigma$ ) of major and trace element (XRF), REE (ICP-EM) and Sr isotope analyses from fresh samples of flow 1 and 9.

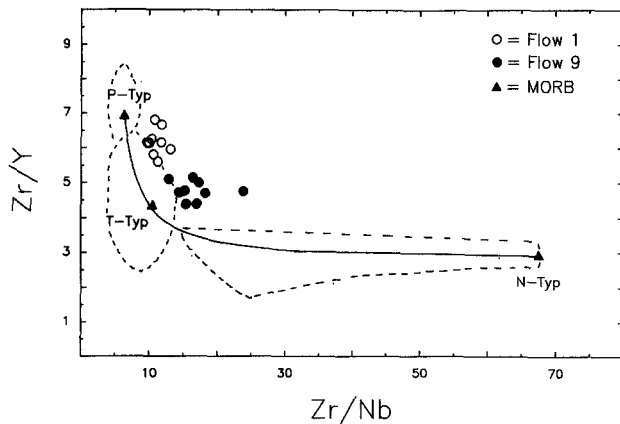


**Fig. 3.** Zr/Y – Zr/Nb variation diagram with a mixing hyperbola between P-, T- and N-type MORB according to LE ROEX (1987). Filled and open circles indicate samples of flow 1 and flow 9 (this paper).

et al. (1983), which shows the low pressure fractionation of quartz-normative tholeiites dominated by plagioclase-clinopyroxene-olivine-( $\pm$  magnetite)-fractionation.

#### Trace elements

With decreasing [Mg]-value from flow 1 to flow 9, the Cr content decreases slightly, while Ni shows little or no depletion. This suggests a weak clinopyroxene fractionation, rather than an extensive olivine fractionation. The Ti/V ratios of between 24 and 32 are MORB-like (LANGMUIR et al., 1977; DUPUY et al., 1988) and the Y/Nb ratios (1.7 for flow 1 and 3.5 for flow 9) are similar to those of T-type MORB (LE ROEX 1987, Y/Nb = 1.2–4.3). The MORB-like composition of these CTs are demonstrated in Fig. 3. In Fig. 4 the within-plate basaltic character of the CTs is revealed. The distinct Zr/Nb, Zr/Y (Fig. 3) and Y/Nb ratios (Fig. 4) of flow 1 and 9 requires a heterogeneous source, because these interelement ratios are not strongly affected by fractionation processes. Further evidence for the heterogeneity of the source is shown by significant differences in the La/Ce, Sm/Nd and Nb/La ratios (Tab. 1). The presence of a crustal type component in some samples is documented by high Rb/Sr ratios (0.09–0.13), low Ti/Zr ratios (59–64) and especially the negative Nb anomaly (DUPUY & DOSTAL 1984) visualized in Fig. 5a.

#### Rare earth elements

The rare earth element (REE) patterns (Fig. 5b) show some typical features for CTs. The

light REE (LREE) enrichment factors (normalised to C1-chondrite after EVENSEN et al., 1978) scatter between 20–50, and those of the heavy REE (HREE) between 5–17. Fig. 6 shows the greater enrichment factors of flow 1 compared to flow 9, suggesting a lower degree of melting and/or a higher crustal contamination of flow 1. The negative Eu anomaly (0.81–0.86) and the Lu enrichment compared to Yb, indicate plagioclase and orthopyroxene fractionation (HENDERSON, 1984), respectively. The Ce enrichment compared to La indicates a clinopyroxene accumulation (HENDERSON, 1984). The similarity of (La/Yb)<sub>N</sub> ratios of different flows (flow 1: 3.6, flow 9: 5.1) excludes an extensive fractionation within the tholeiitic sequence. The shallow HREE pattern indicates no significant fractionation of garnet.

#### Sr isotope data

Analytical data of Rb-Sr isotopes are listed in Tab. 2. Because of the small spread in  $^{87}\text{Rb}/^{86}\text{Sr}$  ratios (< 0.5), the construction of isochrons (even with fresh samples) was not expected. Anyhow,  $^{87}\text{Sr}/^{86}\text{Sr}$  initial ratios and  $\varepsilon_{\text{Sr}}$  – values of flow 1 and 9 (for definition see Tab. 3) could be calculated using the  $^{40}\text{Ar}/^{39}\text{Ar}$  ages. This is possible for these non-metamorphic volcanic rocks because the clo-

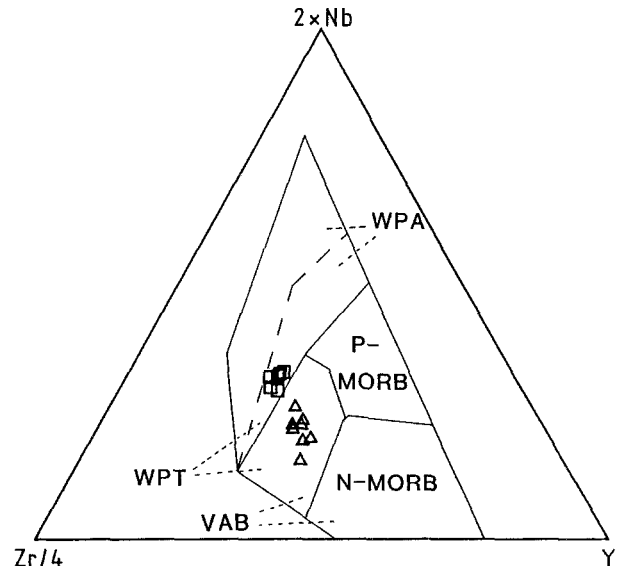


**Fig. 4.**  $2^*\text{Nb} - \text{Zr}/4 - \text{Y}$  tectonomagmatic discrimination diagram for basaltic rocks (MESCHÉDE, 1986). Abbreviations: WPA = within plate alkali basalt; WPT = within plate tholeiite; VAB = volcanic arc basalt; P-MORB = plume type mid-ocean ridge basalt; N-MORB = normal type mid-ocean ridge basalt (squares = fresh samples from flow 1; triangles = fresh samples from flow 9).

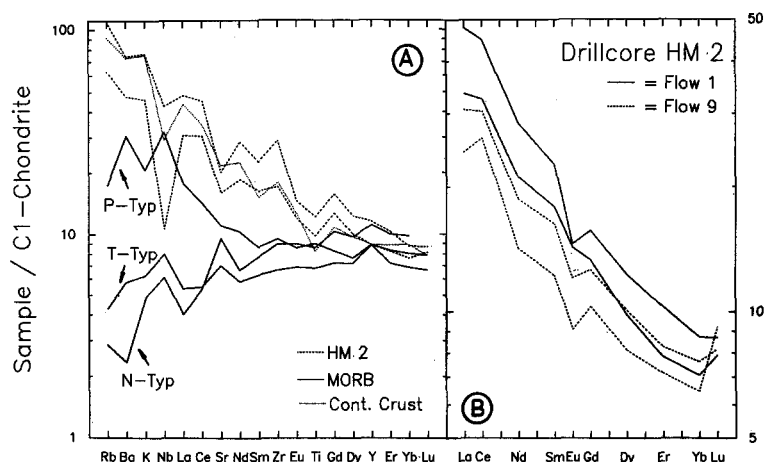


**Fig. 5.** A: Chondrite (C1-) normalized multi-element abundances in HM 2 – tholeiites, MORB (SUN et al., 1979) and continental crust (TAYLOR & McLENNAN, 1985). C1-condrite element abundances from EVENSEN et al. (1978) and THOMPSON et al. (1984) were used for the normalisation of REE and major and trace elements respectively. B: Chondrite (C1-) normalized REE abundances in flow 1 and flow 9 (HM 2), using the normalization constants from EVENSEN et al. (1978).

sure of the system will be contemporaneous with the extrusion and solidification of the lava. The Sr initial ratios ( $0.706640$ ) and  $\epsilon_{\text{Sr}}^t$  values (between  $+30$  and  $+38$ ) are distinctly higher than those of the mantle array which indicates contamination of the tholeiites by a crustal component. Fig. 6 presents a two-component mixing diagram with upper continental crust and MORB as end members. The calculated crustal component proportions for the Rb-Sr system are 17 wt% (flow 1) and 13 wt% (flow 9). The assumption of upper continental crust as one end member, is based on the high contents of large ion lithophile elements (LILE) and the fact that quartz-normative tholeiites are low pressure ( $< 5$  kb) melting derivatives from olivine tholeiites (JAQUES & GREEN, 1980). The MORB composition of the other end member is based on major and trace element contents and element ratios, as discussed above.

It should be noted that the calculated crustal components of flow 1 (17 wt%) and flow 9 (13 wt%) are only approximate estimates. At present, measurements of the Pb isotopes are in progress to quantify and qualify the presence of crustal components more convincingly.

### Alteration

Vesicles in the rocks are filled with secondary phases either with calcite-pumpellyite or pumpellyite-quartz or seldom with epidote-calcite and chlorite is usually present in excess. According to LIU et al. (1987) this parageneses is stable

above  $1.4 \pm 0.5$  Kbar and at above  $228 \pm 30^\circ\text{C}$  and indicate the pressure and temperature conditions during the alteration.

The profile of HM 2 (Fig. 2) shows nine lava flows which can be distinguished by alteration related element mobility. In the altered samples the K- and Rb-contents, the K/Rb- and the Rb/Sr ratios increase significantly (K: 0.83 to 5.70 wt%, Rb: 30 to 130 ppm, K/Rb: 275 to 440, Rb/Sr: 0.12

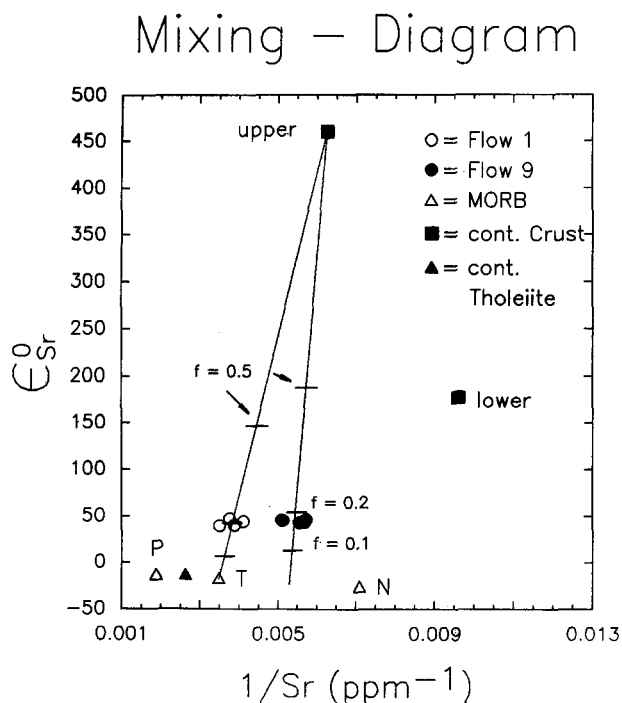


**Fig. 6.**  $\epsilon_{\text{Sr}}^0 - 1/\text{Sr}$  mixing diagram for HM 2 tholeiites compared to MORB (LE ROEX, 1987) and the upper and lower continental crust (FAURE, 1986).

sample	Rb (ppm)	Sr (ppm)	$^{87}\text{Rb}/^{86}\text{Sr}$	$^{87}\text{Sr}/^{86}\text{Sr}$
Fi 98/88 (wr)	13.80	283.50	0.141	0.707270 ± 16
Fi 100/88 (wr)	32.45	265.13	0.352	0.707837 ± 60
Fi 10/88 (wr)	20.05	257.17	0.223	0.707316 ± 19
Fi 13/88 (wr)	12.56	255.92	0.141	0.707363 ± 25
Fi 16/88 (wr)	37.68	242.29	0.442	0.707624 ± 40
Fi 29/88 (wr)	129.08	65.04	5.75	0.720956 ± 30
Fi 30/88 (wr)	142.80	217.35	1.90	0.711360 ± 60
Fi 34/88 (wr)	120.70	68.76	5.09	0.719550 ± 30
Fi 35/88 (wr)	126.90	208.30	1.76	0.710813 ± 60
Fi 36/88 (wr)	144.90	129.80	3.23	0.713689 ± 40
Fi 37/88 (wr)	61.60	258.60	0.689	0.708564 ± 30
Fi 39/88 (wr)	130.12	113.90	3.31	0.713825 ± 50
Fi 40/88 (wr)	92.50	227.25	1.18	0.708970 ± 25
Fi 41/88 (wr)	92.60	66.08	4.06	0.716988 ± 50
Fi 42/88 (wr)	71.18	233.06	0.884	0.708576 ± 30
Fi 44/88 (wr)	129.30	81.09	4.62	0.714632 ± 40
Fi 45/88 (wr)	22.80	291.80	0.226	0.707713 ± 40
Fi 51/88 (wr)	81.70	70.60	3.36	0.715653 ± 40
Fi 52/88 (wr)	39.70	205.19	0.560	0.708880 ± 35
Fi 57/88 (wr)	48.11	71.40	1.95	0.713198 ± 25
Fi 58/88 (wr)	25.07	196.30	0.363	0.707707 ± 18
Fi 63/88 (wr)	24.72	180.29	0.397	0.70753 ± 25
Fi 64/88 (wr)	23.91	174.57	0.393	0.707751 ± 30
Fi 85/88 (wr)	23.25	194.96	0.344	0.707701 ± 30
Fi 88/88 (wr)	23.49	175.86	0.377	0.707548 ± 45
Fi 95/88 (wr)	31.07	256.70	0.350	0.708198 ± 40
Fi 29/88 (m1)	19.56	72.18	0.784	0.712502 ± 25
Fi 34/88 (m1)	41.41	65.66	1.83	0.714405 ± 9
Fi 34/88 (m2)	1.53	130.94	0.0339	0.712359 ± 30
Fi 36/88 (m1)	51.44	78.67	1.89	0.714732 ± 30
Fi 39/88 (m1)	10.94	78.32	0.405	0.711200 ± 25
Fi 39/88 (m2)	0.63	72.34	0.0254	0.710536 ± 30
Fi 41/88 (m1)	62.76	75.58	2.40	0.715322 ± 35
Fi 41/88 (m2)	1.40	68.18	0.0594	0.709727 ± 11
Fi 44/88 (m1)	12.99	64.64	0.582	0.711546 ± 35
Fi 49/88 (m1)	341.03	65.18	15.2	0.736482 ± 45
Fi 51/88 (m1)	142.22	71.60	5.75	0.720566 ± 50
Fi 51/88 (m2)	-	124.07	-	0.708885 ± 35
Fi 57/88 (m2)	0.16	134.58	0.00360	0.708394 ± 45

wr = whole rock

m1 = pumpellyite-chlorite-quartz

m2 = carbonate

Table 2. Sr isotope compositions of whole rocks (wr), pumpellyite-chlorite-quartz mixtures (m1) and carbonates (m2) from the drill core HM 2 samples. Listed error are  $2\sigma$  of the mean.

to 1.66), while the contents of Na, Ca and Sr decrease (Na: 1.33 to 0.37 wt% and Ca: 6.44 to 2.15 wt%, Sr: 250 to 75 ppm). The large Rb contents of altered whole rocks is attributed to the in-

crease of  $\epsilon_{\text{Sr}}^0$  values, and the simultaneous decrease of Sr concentration (Fig. 7). Because of this increase of  $\epsilon_{\text{Sr}}^0$  values with enhanced alteration, the  $\epsilon_{\text{Sr}}^0$  values correlate with the depth of the samples



sample	$(^{87}\text{Sr}/^{86}\text{Sr})_i$	$\epsilon_{\text{Sr}}^0$	$\epsilon_{\text{Sr}}^t$
<b>flow 1:</b>			
Fi 98/88	$0.706848 \pm 20$	+39.9	+36.8
Fi 100/88	$0.706784 \pm 70$	+47.3	+35.9
Fi 10/88	$0.706649 \pm 30$	+39.9	+34.0
Fi 13/88	$0.706942 \pm 30$	+40.6	+38.1
Fi 16/88	$0.706301 \pm 60$	+44.3	+29.0
<b>flow 9:</b>			
Fi 58/88	$0.706656 \pm 25$	+45.5	+33.9
Fi 63/88	$0.70640 \pm 25$	+43.0	+30.3
Fi 64/88	$0.706634 \pm 40$	+46.1	+33.6
Fi 85/88	$0.706722 \pm 40$	+45.4	+34.8
Fi 88/88	$0.706476 \pm 50$	+43.2	+31.6

$$\epsilon_{\text{Sr}}^0 = ((^{87}\text{Sr}/^{86}\text{Sr})_m / (^{87}\text{Sr}/^{86}\text{Sr})_{\text{ur}}^0 - 1) * 10^4$$

$$\epsilon_{\text{Sr}}^t = ((^{87}\text{Sr}/^{86}\text{Sr})_i / (^{87}\text{Sr}/^{86}\text{Sr})_{\text{ur}} - 1) * 10^4$$

with

$$(^{87}\text{Sr}/^{86}\text{Sr})_{\text{ur}} = ((^{87}\text{Sr}/^{86}\text{Sr})_{\text{ur}}^0 - (^{87}\text{Rb}/^{86}\text{Sr})_{\text{ur}}^0 * (e^{\lambda t} - 1))$$

$$m = \text{measured}; (^{87}\text{Sr}/^{86}\text{Sr})_{\text{ur}}^0 = 0.7045; (^{87}\text{Rb}/^{86}\text{Sr})_{\text{ur}}^0 = 0.0816;$$

Table 3.  $(^{87}\text{Sr}/^{86}\text{Sr})_i$ ,  $\epsilon_{\text{Sr}}^0$  and  $\epsilon_{\text{Sr}}^t$  values of fresh samples from flow 1 and 9 (Hm 2).  $^{87}\text{Sr}/^{86}\text{Sr}_i$  ratios were corrected for an age of 210.4 Ma (flow 1) and 200.2 Ma (flow 9).

in the drillcore (Fig. 8). The  $^{87}\text{Sr}/^{86}\text{Sr}$  ratios of secondary carbonates mirror the  $^{87}\text{Sr}/^{86}\text{Sr}$  ratios of alteration fluid(s). Because the  $^{87}\text{Rb}/^{86}\text{Sr}$  ratios of the carbonates are extremely low ( $< 0.06$ ), radiogenic  $^{87}\text{Sr}$  growth cannot be responsible for these  $^{87}\text{Sr}/^{86}\text{Sr}$  ratios. The element mobility and  $^{87}\text{Sr}/^{86}\text{Sr}$

ratios of secondary phases argue against a submarine origin to the alteration. MENZIES & SEYFRIED (1979) and WEDEPOHL (1988) reported K depletion and Na enrichment for submarine altered basalts (temperature of alteration  $> 150^\circ\text{C}$ ). According to FAURE (1982) the seawater  $^{87}\text{Sr}/^{86}\text{Sr}$  ratios decrease

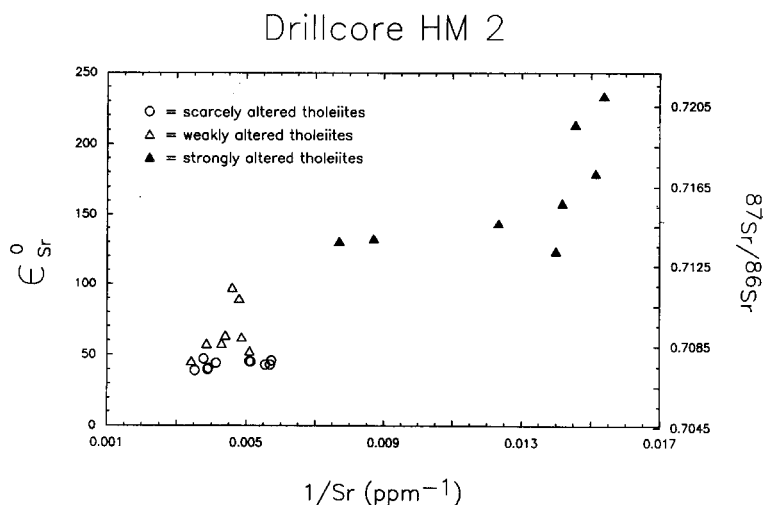
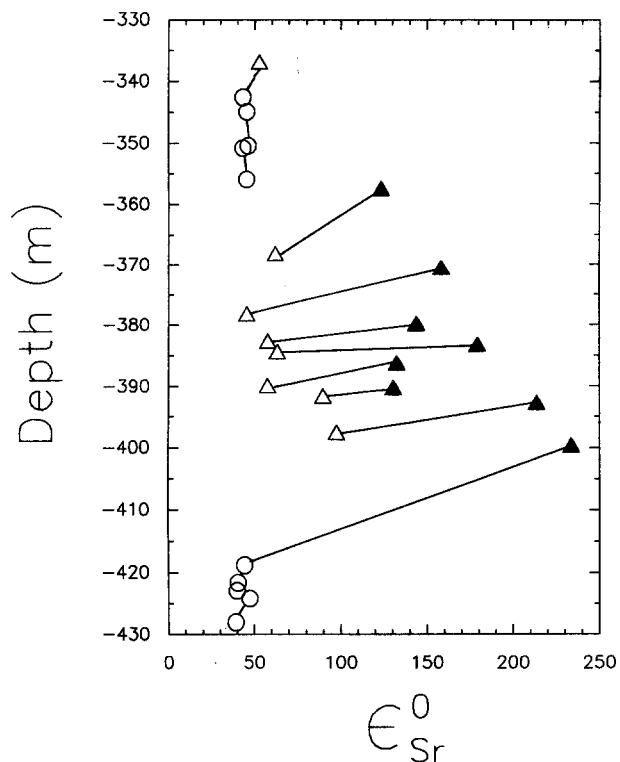


Fig. 7.  $\epsilon_{\text{Sr}}^0 - 1/\text{Sr}$  mixing diagram for the different altered samples of HM 2 tholeiites. With enhancing alteration  $\epsilon_{\text{Sr}}^0$  values increase whereas the Sr-contents decrease.

### Drillcore HM 2



**Fig. 8.** Depth -  $\epsilon_{Sr}^0$  diagram, showing the rapid increase of  $\epsilon_{Sr}^0$  values in the upper strongly altered part of each flow. The symbols are the same as in Fig. 7.

from 0.70773 (220–200 Ma) to 0.70731 (200–180 Ma), thus they are distinctly lower than the observed  $^{87}Sr/^{86}Sr$  ratios in the carbonates. The decrease from 0.7123 (flow 2) to 0.7083 (flow 8) and distinct differences of secondary carbonate  $^{87}Sr/^{86}Sr$  ratios indicate the action of alteration fluids different in chemical composition. The large scatter in  $^{87}Rb/^{86}Sr$  and  $^{87}Sr/^{87}Sr$  ratios of the secondary minerals compared to the whole rock data indicate isotopic disequilibrium in the secondary minerals. This suggests that the fluid/rock reactions causing the alteration proceeded rapidly.

### Geochronology

The measured and calculated Ar isotope ratios and the age values of the samples are listed in Tab. 4. Traditionally, the data are represented as age spectra which are constructed assuming that the difference between the measured and neutron induced argon isotope interferences at mass  $^{36}Ar$  gives the amount of atmospheric  $^{36}Ar$ . Therefore, the radiogenic  $^{40}Ar$  content of a degassing step is calculated from the measured  $^{40}Ar$  content reduced by a factor of 295.5 times the atmospheric  $^{36}Ar$  value assuming that atmospheric argon was incorporated into the minerals when the system became closed. However, if the initial ratio is not

Temp °C	$^{40}Ar \cdot 10^{-8}$ (cc STP/g)	$^{40}Ar/^{36}Ar$	$^{39}Ar/^{40}Ar$	$^{39}Ar/^{37}Ar$	$^{40}Ar$ rad (%)	$^{39}Ar$ (%) released	$^{40}Ar$ rad/ $^{39}Ar_k$	Age (Ma)
Fi 16/88, Plagioclase, drill core HM 2, bottom flow, weight: 98.59 mg, J-value: 0.02129 ± 0.00067								
500	22.90 ± 1.15	318.9 ± 14.1	0.0130 ± 0.0002	0.140 ± 0.002	7.3 ± 4.1	0.92	5.70 ± 3.15	205. ± 108
610	9.37 ± 0.50	435.5 ± 62.5	0.0590 ± 0.0006	0.0560 ± 0.0005	32.1 ± 10.0	2.84	5.44 ± 1.60	198. ± 60
715	27.5 ± 1.4	1125.0 ± 105.5	0.1167 ± 0.0007	0.04542 ± 0.00010	73.7 ± 2.5	12.62	6.315 ± 0.214	227.6 ± 9.9
800	34.1 ± 1.7	9800 ± 6960	0.1655 ± 0.0009	0.04567 ± 0.00010	97.0 ± 2.0	30.13	5.860 ± 0.135	212.2 ± 7.8
860	32.7 ± 1.6	11200 ± 9120	0.1690 ± 0.0010	0.0476 ± 0.0001	97.4 ± 2.0	47.30	5.761 ± 0.130	208.8 ± 7.8
940	31.48 ± 1.60	5400 ± 2050	0.1655 ± 0.0009	0.04967 ± 0.00010	94.6 ± 2.0	63.47	5.731 ± 0.130	207.1 ± 7.6
990	25.3 ± 1.3	3970 ± 1100	0.1616 ± 0.0009	0.05329 ± 0.00010	92.6 ± 2.0	76.19	5.728 ± 0.130	207.6 ± 7.7
1050	24.0 ± 1.2	3180 ± 812	0.1603 ± 0.0009	0.04554 ± 0.00020	97.0 ± 2.0	88.13	5.657 ± 0.150	205.2 ± 8.0
1150	13.55 ± 0.70	2080 ± 505	0.1412 ± 0.0009	0.04757 ± 0.00020	85.8 ± 3.0	94.07	6.07 ± 0.25	219.5 ± 10.6
1250	13.3 ± 6.6	2200 ± 360	0.1434 ± 0.0009	0.0437 ± 0.0002	86.6 ± 3.0	100.00	6.04 ± 0.25	218.2 ± 10.2
Total	234. ± 12	1500 ± 360	0.1375 ± 0.0008	0.04789 ± 0.00007	80.27 ± 0.90		5.838 ± 0.070	211.4 ± 6.8
Fi 64/88, Plagioclase, drill core HM 2, top flow, weight: 94.15 mg, J-value: 0.02129 ± 0.00067								
500	43.7 ± 2.2	327.4 ± 8.7	0.01207 ± 0.00010	0.6850 ± 0.0160	9.7 ± 2.4	1.01	8.1 ± 2.0	286. ± 65
610	16.19 ± 0.80	395 ± 35	0.03090 ± 0.00025	0.2670 ± 0.0030	25.1 ± 6.6	1.98	8.1 ± 2.1	288. ± 70
715	32.38 ± 1.60	1013 ± 90	0.1168 ± 0.0005	0.1131 ± 0.0003	70.8 ± 2.6	9.26	6.07 ± 2.25	219.2 ± 10.1
800	48.2 ± 2.4	2330 ± 280	0.1560 ± 0.0007	0.07461 ± 0.00016	87.33 ± 1.50	23.75	5.56 ± 0.10	203.2 ± 7.0
860	85.6 ± 4.3	5650 ± 1270	0.1706 ± 0.0008	0.08782 ± 0.00019	94.77 ± 1.18	51.88	5.554 ± 0.070	201.7 ± 6.6
940	54.9 ± 2.7	4640 ± 900	0.1678 ± 0.0007	0.09453 ± 0.00020	93.63 ± 1.25	69.62	5.581 ± 0.080	202.6 ± 6.6
990	43.6 ± 2.2	3780 ± 640	0.1671 ± 0.0007	0.1286 ± 0.0003	92.18 ± 1.30	83.65	5.515 ± 0.080	200.3 ± 6.6
1050	27.29 ± 1.40	2050 ± 310	0.1513 ± 0.0007	0.1479 ± 0.0004	88.60 ± 2.19	91.61	5.657 ± 0.145	205.2 ± 7.9
1150	17.16 ± 0.90	1030 ± 160	0.1241 ± 0.0006	0.06618 ± 0.00019	71.3 ± 4.3	95.71	5.75 ± 0.35	208.4 ± 13.4
1250	18.46 ± 0.18	690 ± 110	0.1204 ± 0.0006	0.04842 ± 0.00016	57.1 ± 5.6	100.00	4.74 ± 0.45	173.5 ± 17.1
total	388. ± 19	1200 ± 110	0.1339 ± 0.0006	0.09216 ± 0.00011	75.4 ± 7.0		5.629 ± 0.060	204.2 ± 6.4

Temp °C	$^{40}\text{Ar} \times 10^{-8}$ (cc STP/g)	$^{40}\text{Ar}/^{36}\text{Ar}$	$^{39}\text{Ar}/^{40}\text{Ar}$	$^{39}\text{Ar}/^{37}\text{Ar}$	$^{40}\text{Ar}$ rad (%)	$^{39}\text{Ar}$ (%) released	$^{40}\text{Ar}_{\text{rad}}/^{39}\text{Ar}_{\text{K}}$	Age (Ma)
Fi 78/88, Plagioclase, sw' Haut Moulouya, weight : 89.13 mg, J-value : 0.02129 ± 0.00067								
500	27.40 ± 1.40	373.8 ± 21.3	0.03209 ± 0.00020	0.1183 ± 0.0006	23.0 ± 4.5	2.95	6.53 ± 1.40	235. ± 48
610	18.75 ± 0.90	1115 ± 150	0.1304 ± 0.0006	0.07435 ± 0.00018	73.5 ± 3.7	11.16	5.64 ± 0.30	204.6 ± 11.5
715	27.34 ± 1.40	1263 ± 160	0.1552 ± 0.0007	0.05672 ± 0.00014	76.6 ± 3.0	25.41	4.937 ± 0.190	180.4 ± 8.6
800	37.8 ± 1.9	2870 ± 480	0.1721 ± 0.0007	0.06437 ± 0.00015	89.71 ± 1.70	47.27	5.213 ± 0.103	189.9 ± 6.7
860	19.17 ± 1.00	4516 ± 1180	0.1657 ± 0.0007	0.07888 ± 0.00019	93.46 ± 1.70	57.94	5.638 ± 0.106	204.6 ± 7.1
940	14.61 ± 0.70	1920 ± 520	0.1583 ± 0.0007	0.1002 ± 0.0003	84.6 ± 4.2	65.71	5.35 ± 0.25	194.5 ± 10.8
990	29.23 ± 1.50	1542 ± 190	0.1648 ± 0.0007	0.09532 ± 0.00025	80.8 ± 2.4	81.89	4.906 ± 0.145	179.3 ± 7.4
1050	15.37 ± 0.80	2180 ± 580	0.1500 ± 0.0006	0.07609 ± 0.00019	86.4 ± 3.6	89.63	5.76 ± 0.25	208.9 ± 10.3
1150	9.22 ± 0.50	1180 ± 320	0.1160 ± 0.0006	0.05295 ± 0.00020	74.9 ± 6.8	93.50	6.46 ± 0.60	233. ± 21
1250	15.50 ± 0.80	1006 ± 160	0.1248 ± 0.0006	0.04817 ± 0.00013	70.6 ± 4.9	100.00	5.66 ± 0.40	205.3 ± 14.2
total	215.1 ± 10.8	1153 ± 90	0.1384 ± 0.0006	0.07050 ± 0.00008	74.36 ± 1.1		5.373 ± 0.080	195.5 ± 6.5
Fi 5/88, Plagioclase, w' High Atlas, weight: 96.81 mg, J-value : 0.02129 ± 0.00067								
500	20.12 ± 1.00	342 ± 20	0.02073 ± 0.00016	0.2418 ± 0.0025	13.8 ± 5.2	1.00	6.6 ± 2.5	238. ± 85
610	13.44 ± 0.70	756 ± 135	0.08932 ± 0.00050	0.08735 ± 0.00045	60.9 ± 7.0	3.88	6.82 ± 0.80	245. ± 27
715	39.26 ± 2.00	2520 ± 325	0.1489 ± 0.0005	0.07355 ± 0.00016	88.25 ± 1.50	17.93	5.927 ± 0.104	214.4 ± 7.3
800	68.3 ± 3.4	2530 ± 290	0.1605 ± 0.0006	0.07831 ± 0.00015	88.31 ± 1.35	44.27	5.503 ± 0.090	199.9 ± 6.7
860	48.2 ± 2.4	2800 ± 370	0.1601 ± 0.0006	0.08822 ± 0.00025	89.45 ± 1.40	62.81	5.587 ± 0.090	202.8 ± 6.8
940	28.33 ± 1.40	3160 ± 570	0.1520 ± 0.0005	0.1281 ± 0.0003	90.66 ± 1.70	73.15	5.966 ± 0.113	215.8 ± 7.5
990	28.39 ± 1.40	1528 ± 190	0.1496 ± 0.0005	0.1294 ± 0.0003	80.6 ± 2.3	83.17	5.489 ± 0.160	199.5 ± 8.1
1050	17.19 ± 0.90	1450 ± 240	0.1368 ± 0.0005	0.07451 ± 0.00018	79.6 ± 3.4	88.82	5.82 ± 0.25	210.8 ± 10.5
1150	17.93 ± 0.90	907 ± 11	0.1256 ± 0.0005	0.05426 ± 0.00015	67.4 ± 4.0	94.23	5.37 ± 0.30	195.3 ± 12.5
1250	19.29 ± 1.00	1387 ± 180	0.1245 ± 0.0005	0.04767 ± 0.00012	78.7 ± 2.7	100.00	6.32 ± 0.20	227.8 ± 10.0
total	300.5 ± 15.0	1435 ± 100	0.1385 ± 0.0005	0.08134 ± 0.00009	79.41 ± 7.70		5.732 ± 0.060	207.8 ± 6.5
Fi 7/88, Plagioclase, w' High Atlas, weight: 103.35 mg, J-value : 0.02129 ± 0.00067								
610	7.47 ± 0.40	761 ± 145	0.1059 ± 0.0006	0.02990 ± 0.00011	61.2 ± 7.3	8.24	5.77 ± 0.70	209. ± 25
715	20.07 ± 1.00	2370 ± 710	0.1559 ± 0.0007	0.02552 ± 0.00006	87.5 ± 3.7	33.02	5.61 ± 0.25	203.7 ± 10.3
800	18.43 ± 0.90	5200 ± 3470	0.1527 ± 0.0007	0.02414 ± 0.00006	94.3 ± 3.8	55.30	6.18 ± 0.25	223.0 ± 10.7
860	10.72 ± 0.50	934 ± 145	0.1381 ± 0.0007	0.02438 ± 0.00008	68.4 ± 4.9	67.02	4.95 ± 0.35	180.8 ± 13.5
940	7.30 ± 0.40	4700 ± 2750	0.1272 ± 0.0007	0.02505 ± 0.00010	93.7 ± 3.6	74.37	7.37 ± 0.30	263.1 ± 12.4
990	5.05 ± 0.25	26000 ± 70000	0.1288 ± 0.0009	0.02510 ± 0.00015	98.9 ± 3.2	79.52	7.67 ± 0.25	273.1 ± 11.6
1100	10.20 ± 0.50	964 ± 180	0.1208 ± 0.0006	0.02568 ± 0.00009	69.4 ± 5.6	89.28	5.74 ± 0.50	208.1 ± 17.1
1250	13.44 ± 0.70	600 ± 60	0.1007 ± 0.0005	0.02476 ± 0.00009	50.7 ± 5.0	100.00	5.04 ± 0.50	184.0 ± 17.9
total	100.5 ± 5.0	1030 ± 296	0.1257 ± 0.0005	0.02548 ± 0.00003	71.37 ± 1.80		5.676 ± 0.145	205.9 ± 7.9
Fi 111/88, Plagioclase, s' Middle Atlas, weight : 94.14 mg, J-value : 0.02129 ± 0.00067								
500	34.10 ± 1.70	311.0 ± 8.2	0.02544 ± 0.00020	0.1831 ± 0.0013	5.0 ± 2.5	2.06	1.96 ± 1.00	74. ± 35
610	24.64 ± 1.20	595 ± 30	0.08946 ± 0.00050	0.06732 ± 0.00020	50.3 ± 2.7	7.30	5.62 ± 0.30	204.0 ± 12.1
715	26.59 ± 1.30	1650 ± 209	0.1581 ± 0.0009	0.08026 ± 0.00020	82.1 ± 2.3	17.30	5.194 ± 0.145	189.3 ± 7.6
800	42.1 ± 2.1	3400 ± 609	0.1688 ± 0.0009	0.07867 ± 0.00019	91.32 ± 1.60	34.20	5.41 ± 0.10	196.7 ± 6.8
860	28.51 ± 1.45	5050 ± 1280	0.1723 ± 0.0009	0.08881 ± 0.00025	94.14 ± 1.50	45.89	5.463 ± 0.090	198.5 ± 6.7
940	33.69 ± 1.70	1990 ± 206	0.1703 ± 0.0009	0.1055 ± 0.0002	85.16 ± 1.50	59.53	5.002 ± 0.090	182.6 ± 6.4
990	37.76 ± 1.90	1131 ± 100	0.1435 ± 0.0008	0.08975 ± 0.00020	73.9 ± 2.2	72.42	5.148 ± 0.160	187.7 ± 7.8
1050	38.78 ± 1.90	708 ± 35	0.1040 ± 0.0006	0.06674 ± 0.00018	58.2 ± 2.1	82.01	5.601 ± 0.200	203.3 ± 9.2
1150	41.2 ± 2.1	778 ± 40	0.1083 ± 0.0006	0.06234 ± 0.00015	62.03 ± 1.80	92.63	5.727 ± 0.170	207.6 ± 8.6
1250	27.54 ± 1.40	839 ± 70	0.1124 ± 0.0006	0.05250 ± 0.00014	64.8 ± 2.9	100.00	5.76 ± 0.25	208.8 ± 10.6
total	334.9 ± 16.8	890 ± 50	0.1255 ± 0.0007	0.07767 ± 0.00008	66.61 ± 0.70		5.323 ± 0.060	193.7 ± 6.2
Corrections for interferences:								
rad	: radiogenic							
K	: neutron produced from K only							
\	: 5.543 10 <sup>-10</sup> a <sup>-1</sup> (STEIGER and JÄGER, 1979)							
Standard LP-6	: K 8.33 ± 3 %							
	Ca 0.077 %							
	age 128.9 Ma							
	$^{36}\text{Ar}/^{37}\text{Ar}(\text{Ca})$	=	2.7 ± 0.2 10 <sup>-4</sup>	STETTLER et al., 1973				
	$^{38}\text{Ar}/^{37}\text{Ar}(\text{Ca})$	=	6.0 ± 2.0 10 <sup>-5</sup>	STETTLER et al., 1973				
	$^{39}\text{Ar}/^{37}\text{Ar}(\text{Ca})$	=	6.8 ± 0.2 10 <sup>-4</sup>	STETTLER et al., 1973				
	$^{40}\text{Ar}/^{37}\text{Ar}(\text{Ca})$	=	6.0 ± 2.0 10 <sup>-3</sup>	STETTLER et al., 1973				
	$^{40}\text{Ar}/^{39}\text{Ar}(\text{K})$	=	3.0 ± 3.0 10 <sup>-4</sup>	TURNER et al., 1973				
	$^{36}\text{Ar}/^{39}\text{Ar}(\text{K})$	=	1.4 ± 0.3 10 <sup>-2</sup>	MAURER, 1973				

Table 4. Argon isotope compositions of plagioclase phenocrysts.

equal to the atmospheric value, in the presence of excess argon for example, the above reduction methodology leads to age estimates that are too old. Fortunately, the  $^{39}\text{Ar}/^{40}\text{Ar}$  vs  $^{36}\text{Ar}/^{40}\text{Ar}$  diagram circumvents this difficulty and measured ratios only fit a straight line if the Ar isotope ratios were generated by two end members. The end members are given by the intercepts on the abscissa ( $^{36}\text{Ar}/^{40}\text{Ar}$ ) and the ordinate ( $^{39}\text{Ar}/^{40}\text{Ar}$ ). The  $^{36}\text{Ar}/^{40}\text{Ar}$  intercept represents the initial ratio when the mineral became a closed system. Usually the reciprocal of it is equal to 295.5. The  $^{39}\text{Ar}/^{40}\text{Ar}$  intercept is given by the radiogenic amounts of  $^{40}\text{Ar}$  due to the in situ radioactive decay and the neutron induced conversion of  $^{39}\text{K}$  to  $^{39}\text{Ar}$ . The reciprocal of this ratio is proportional to the age of the degassing step and here it is called intercept age. If the reciprocal of the x-axis intercept is greater than 295.5, excess argon has to be considered. In the following discussion we compare the plateau age given by the age spectrum with the intercept age. The mixing line was calculated by cubic regression according to a treatment given by Brooks et al. (1972).

## Results

Six separates of translucent plagioclase phenocrysts from the continental tholeiites yield meaningful geological ages. In the case of two samples (Fi 16/88 and Fi 64/88, drillcore HM 2) excellent plateau ages were derived, presumably a result of the extreme purity of the minerals. Under the microscope, no inclusions and alterations effects were detected. In contrast, the other four samples were slightly altered (secondary phases), which leads to poorly defined and disturbed age spectra, but nevertheless their total degassing ages are significant in the geological context.

### Drillcore samples (Fi 16/88 and Fi 64/88)

The plagioclase samples from the drillcore, Fi 16/88 comes from the bottom (approx. 419 m below surface) and Fi 64/88 from the top (approx. 350 m below surface), are representatives of flow 1 and flow 9. They yield excellent plateau ages of  $208.2 \pm 2.3$  Ma and  $203.6 \pm 2.6$  Ma, respectively (Fig. 9). In both cases the plateau ages are defined by five degassing steps (800, 860, 940, 990 and  $1050^\circ\text{C}$ ) which covered more than 80% of  $^{39}\text{Ar}$  released. Fig. 9 reveals that the difference between these plateau ages lies within the  $1\sigma$  error limits.

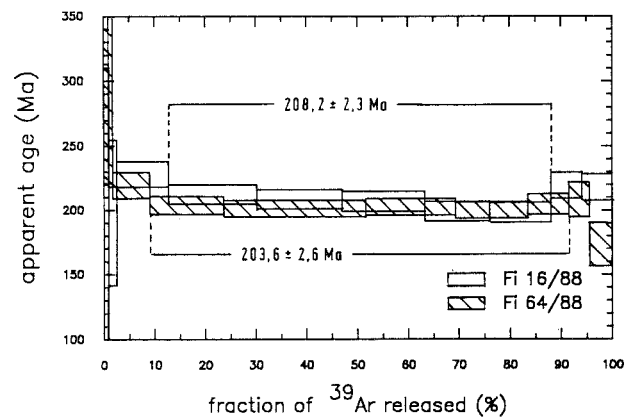


Fig. 9. Age spectra for plagioclases of Fi 16/88 (flow 1 of HM 2) with a plateau age of  $208.2 \pm 2.3$  Ma and of Fi 64/88 (flow 9 of HM 2) with a plateau age of  $203.6 \pm 2.6$  Ma.

But nevertheless the plagioclase of flow 1 is slightly older than those of flow 9.

Evaluating the measured ratios in more detail, the data of the plateau steps of the two samples are presented  $^{39}\text{Ar}/^{40}\text{Ar}$  vs  $^{36}\text{Ar}/^{40}\text{Ar}$  diagram shown in Fig. 10. Bot samples (Fi 16/88 and Fi 64/88) yield a MSWD value (mean standard weighted deviates) of 2.02, and 1.02 respectively. The initial intercept of Fi 16/88 corresponds to a  $^{40}\text{Ar}/^{36}\text{Ar}$  ratio of  $220 \pm 50$  resulting from isotope fractionation, due to preferential leakage of  $^{36}\text{Ar}$  in one valve of the extraction and purification system. The effect on the age value is negligible. The intercept age lead to a value of  $211.8 \pm 2.1$  Ma. Correcting the plateau age values for the low initial ratio, the age values decrease to  $210.4 \pm 2.1$  Ma.

The reciprocal of the x-axis intercept ( $^{40}\text{Ar}/^{36}\text{Ar} = 330 \pm 15$ ) from sample Fi 64/88 (flow 9) gives a small, but negligible excess component, which does not affect the age value ( $200.2 \pm 1.0$  Ma) significantly.

The time span between the bottom (flow 1 and the top (flow 9) of this lava flow sequence is about  $10 \pm 2$  Ma.

### High Atlas samples (Fi 5/88 and Fi 7/88)

The age spectrum of Fi 5/88 yields a plateau age of  $207.8 \pm 6.5$  Ma. Slight variations in the  $^{40}\text{Ar}^*/^{39}\text{Ar}_K$  ratios of the high temperature steps (Fig. 11) lie within the  $2\sigma$ -confidence level, and thus are part of the plateau (McINTYRE 1963, DALRYMPLE & LANPHERE, 1969).

In the correlation diagram ( $^{39}\text{Ar}/^{40}\text{Ar}$  vs  $^{36}\text{Ar}/^{40}\text{Ar}$ ) the data points of the plateau steps scatter

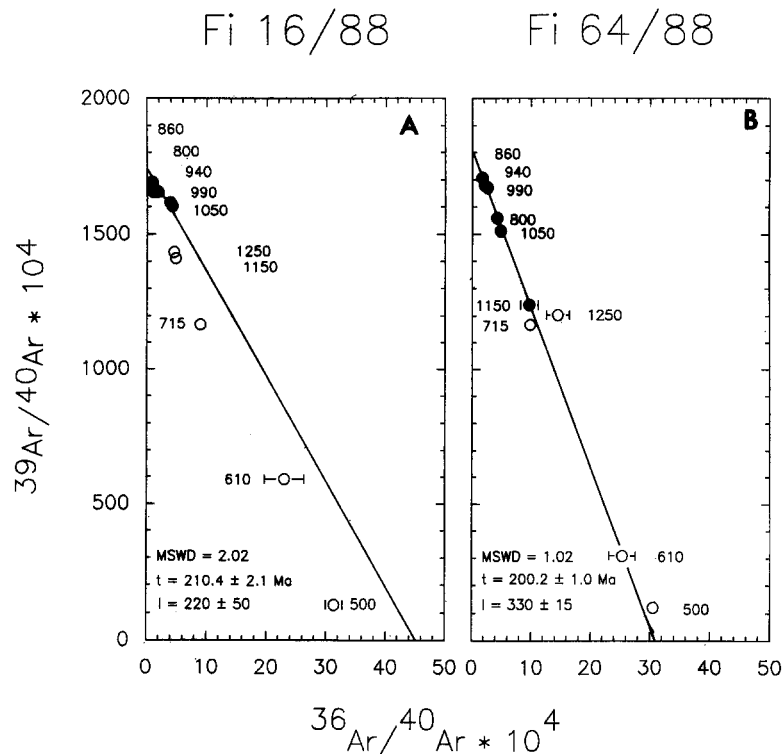


**Fig. 10.**  $^{39}\text{Ar}/^{40}\text{Ar}$  vs.  $^{36}\text{Ar}/^{40}\text{Ar}$  isotope correlation diagrams for plagioclases of Fi 16/88 (a) and Fi 64/88 (b). The age values derived from these diagrams are within the error limit the same as in fig. 9. The data points are labelled with the degassing temperatures. Only data points indicated with black dots are used in the regression (Brooks et al., 1972) analyses.

around a mixing line with a MSDW index of 6.34 indicating the bad correlation of the data. Of only four plateau steps (800, 860, 990 and 1150°C) the mixing line has a MSDW index of 1.12 and yields an intercept age of  $203.3 \pm 2.6$  Ma. The other plateau steps (940, 1050°C) lie on another mixing line, with the same X-intercept (corresponding  $^{40}\text{Ar}/^{36}\text{Ar} = 269 \pm 20$ ) but a higher intercept age of 218 Ma. The meaning of this result is discussed together with that of sample Fi 78/88 further below.

The K-Ar system of Fi 7/88 is strongly disturbed, indicating an age spectrum with great variations in the  $^{40}\text{Ar}^*/^{39}\text{Ar}_K$  ratios (Fig. 11). However, the total degassing age of Fi 7/88 is  $205.9 \pm 7.9$  Ma and seems to be significant in the geological context. Because of the scattering of data points, mixing lines (Fig. 12b) have not been calculated.

#### Haute Moulouya (Fi 78/88) and Middle Atlas (Fi 111/88)

The age spectrum of Fi 78/88 yielded no plateau age (Fig. 13), because of significant variations in the  $^{40}\text{Ar}^*/^{39}\text{Ar}_K$  ratios. The data points of Fi 78/

88 show an interesting feature in the  $^{39}\text{Ar}/^{40}\text{Ar}$  vs  $^{36}\text{Ar}/^{40}\text{Ar}$  diagram (Fig. 14). The three calculated lines (610, 860, 1050, 1150, 1250°C; 715, 990°C, and 800, 940°C) have the same reciprocal X-intercept of  $345 \pm 50$  but different Y-intercepts with corresponding intercept ages of  $202.2 \pm 4.2$ ,  $192.8 \pm 1.1$  and  $174.2 \pm 1.2$  Ma, respectively. The higher  $^{39}\text{Ar}/^{40}\text{Ar}$  ratios could be a result of radiogenic  $^{40}\text{Ar}$  loss due to diffusion or a result of  $^{39}\text{Ar}$  gain due to redistributed  $^{39}\text{Ar}$  by recoil effects dur-

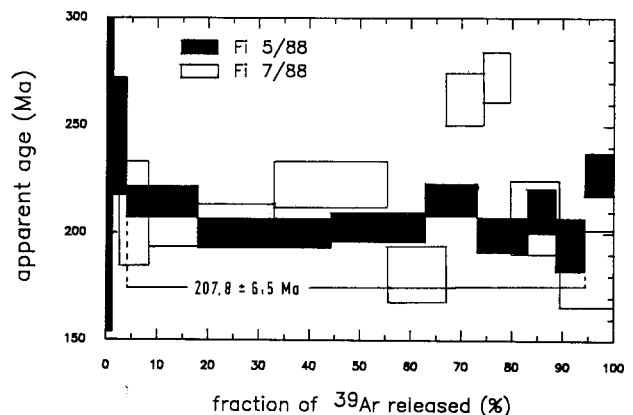


**Fig. 11.** Age spectra for plagioclases of Fi 5/88 and Fi 7/88. Only Fi 5/88 give a reasonable plateau age of  $207.8 \pm 6.5$  Ma.

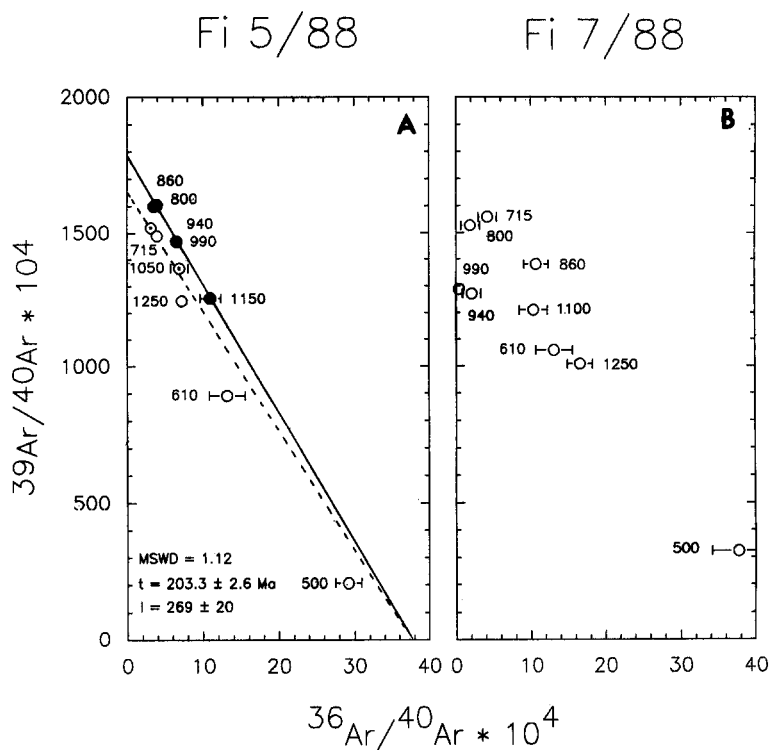


**Fig. 12.**  $^{39}\text{Ar}/^{40}\text{Ar}$  vs.  $^{36}\text{Ar}/^{40}\text{Ar}$  isotope correlation diagrams for plagioclases of Fi 5/88 (a) and Fi 7/88 (b). For discussion see text.

ing the irradiation. Radiogenic argon loss is considered to be associated with a stair-case age pattern, where the low temperature degassing steps result in low apparent ages. But this behaviour is not observed with this sample. The non-systematic disturbance of the age spectrum supports the idea of  $^{39}\text{Ar}$  gain induced by the recoil effect. Recoil transfer  $^{39}\text{Ar}$  from less retentive lattice sites to more retentive sites, which leads to  $^{39}\text{Ar}$  gain, is described as the recoil effect. According to HUNNECKE & SMITH (1976), recoil effects dominate the age spectrum only when potassium rich and potassium poor mineral phase exist together. And indeed, exsolution phenomenon of plagioclase are well known of submicroscopic intergrowth of sodium-rich and calcium-rich domains. It may be that the potassium contents of these domains are different which would cause recoil effects of  $^{39}\text{Ar}$ . The same behaviour can be observed in sample Fi 5/88 (Fig. 12a) of the 750 and 1050°C degassing steps as indicated in the  $^{39}\text{Ar}/^{40}\text{Ar}$  vs  $^{36}\text{Ar}/^{40}\text{Ar}$  diagram. It seems possible to distinguish between  $^{40}\text{Ar}$  loss and a recoil related  $^{39}\text{Ar}$  redistribution. However, the total degassing age of sample Fi 78/88 is again meaningful in the geological context, because  $^{39}\text{Ar}$  loss from the whole system is subordinate.

The age spectrum of Fi 111/88 could be subdivided into two segments, both with a  $^{40}\text{Ar}^*$  loss in lower temperature steps (Fig. 13). The high temperature steps of each segment (800, 860°C and 1050, 1150, 1250°C) yield »plateaus« with ages of  $197.6 \pm 6.5 \text{ Ma}$  and  $206.5 \pm 9.5 \text{ Ma}$  respectively. The subdivided age spectrum could be related to albite-twinning, where  $^{40}\text{Ar}$  loss by diffusion occurred along the composition plane of the minerals. In the  $^{39}\text{Ar}/^{40}\text{Ar}$  vs  $^{36}\text{Ar}/^{40}\text{Ar}$  diagram (Fig. 14) the

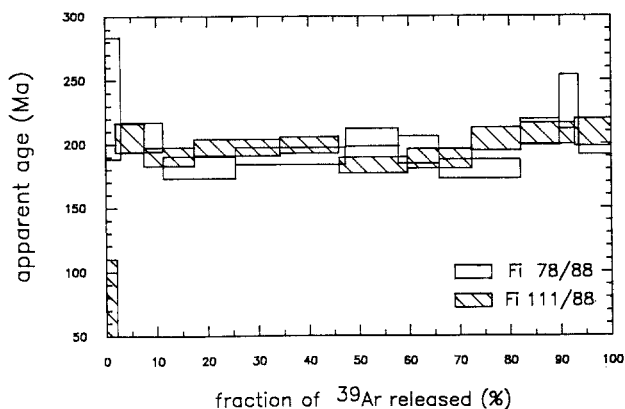


**Fig. 13.** Age spectra for plagioclases of Fi 78/88 and Fi 111/88. The total degassing ages are  $195.5 \pm 6.5 \text{ Ma}$  and  $193.7 \pm 6.2 \text{ Ma}$ , respectively.

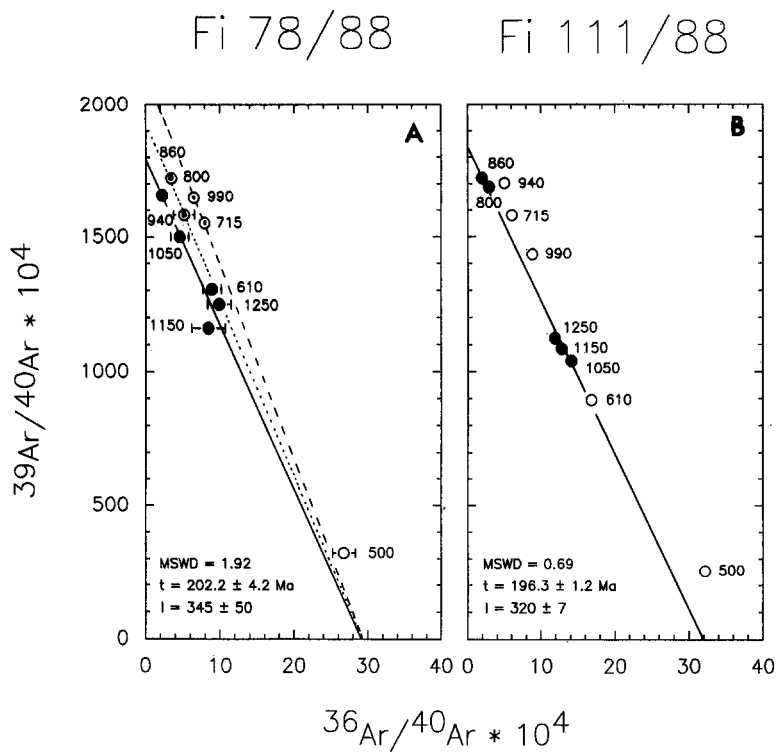


Fig. 14.  $^{39}\text{Ar}/^{40}\text{Ar}$  vs.  $^{36}\text{Ar}/^{40}\text{Ar}$  isotope correlation diagrams for plagioclases of Fi 78/88 (a) and Fi 111/88 (b). For discussion see text.

stage	age (Ma)	I		II		III			IV
		MA	HA	MA	HA	MA	HA	HM	
Bathonian	-170±4								
Bajocian									
Aalénian	-178±4								
Toarcian	-181	-182 ± 13							
Pliensbachian	-189			-190 ± 13					
Sinemurian	-195		196 ± 17			-196.3 ± 1.2			
Hettangian	-201	-199 ± 15	197 ± 13				203.3 ± 2.6	200.2 ± 1.1	
Rhaetian	-204±4			205 ± 17			205.9 ± 7.9		
Norian	-210-?			-208 ± 15	206 ± 13			210.4 ± 2.1	
Karnian	-220±8								
Ladinian	-229±5								

Table 5. Comparison of stratigraphic versus radiometric age values of different lava flows from Morocco according to different authors. I. K-Ar ages after MANSPEIZER et al. (1978) with  $^{40}\text{K}/\text{K} = 1.22 \times 10^{-4}$ ,  $\lambda_B = 4.72 \times 10^{-10} \text{ a}^{-1}$ ,  $\lambda_C = 0.585 \times 10^{-10} \text{ a}^{-1}$ ; II. recalculated K-Ar ages of I (using constants recommended by STEIGER & JÄGER 1977); III.  $^{40}\text{Ar}/^{39}\text{Ar}$ -ages (this paper); IV. stratigraphically required ages (COUSMINER & MANSPEIZER, 1976; WARME, 1988; HAUPTMANN, 1990). Abbreviations: HA = High Atlas, MA = Middle Atlas, HM = Haute Moulouya.

five data points of the »plateaus« yield a mixing line with a MSWD index of 0.69. The reciprocal X- and Y-intercepts correspond to a  $^{40}\text{Ar}/^{36}\text{Ar}$  ratio of  $320 \pm 7$  and an age of  $196.3 \pm 1.2$  Ma respectively, which appears geologically meaningful.

### Discussion

The contents of compatible elements from the CTs are similar to MORB, indicating a source composition of subcontinental and suboceanic mantle. Therefore, high LILE contents and Sr isotope characteristics evidence contamination by a crustal component. These two features agree with the models of ALLÉGRE et al. (1982), CARTER et al. (1978), DUPUY & DOSTAL (1984), HERGT et al. (1989), MENZIES et al. (1983) and STETTLER & ALLÉGRE (1979), which describe a MORB-like mantle and a crustal component for CT genesis.

The subaerial lava flows indicate rapid cooling and, in connection with the low closure temperature of  $200 \pm 50^\circ\text{C}$  (BERGER & YORCK, 1981) for plagioclase, the reported age values have to be interpreted as extrusion ages. Translucent plagioclase crystals gave well defined plateau ages whereas the milky plagioclase phenocrysts yielded disturbed age spectra. The  $^{39}\text{Ar}/^{40}\text{Ar}$  vs  $^{36}\text{Ar}/^{40}\text{Ar}$  diagram reveals some interesting aspects such as excess argon, and  $^{39}\text{Ar}$  redistribution by recoil during the neutron activation. The highest age of  $210.4 \pm 2.1$  Ma and the lowest age of  $200.2 \pm 1.0$  Ma from the drillcore samples indicate the lava sequence of about 100 m was extruded within 10 Ma. This is in good agreement with the stratigraphic stage according to ODIN et al. (1982) and COWIE & BASSETT (1989).

In addition to the Ar-data presented here, there are the published K-Ar ages (whole rock and felspar) for the Atlas system by MANSPEIZER et al. (1978). These K-Ar ages range between  $199 \pm 15$  Ma and  $182 \pm 13$  Ma, which corresponds to a period of Lower Sinemurian to Upper Toarcian (ODIN et al., 1982; COWIE & BASSETT, 1989). The discrepancy between the age data of the present work and those of MANSPEIZER et al. (1978) results from use of different decay constants and isotope ratios. Recalculating MANSPEIZER's data with the decay constants and isotope ratios recommended by STEIGER & JÄGER (1977), there is good agreement (Tab. 5) with the  $^{40}\text{Ar}/^{39}\text{Ar}$  ages (this paper) and the biostratigraphic position of the tholeiites. For the underlying continental redbed sediments, COUSMINER & MANSPEIZER (1976) published a middle Carnian age. Marine Sinemurian sedi-

ments (WARME, 1988; HAUPTMANN, 1990) overlie the early Mesozoic volcanics.

Comparing the tholeiites from Morocco with tholeiites and dolerites from the circum-Atlantic area (Spain and Portugal: Messejana Dyke  $166\text{--}194$  Ma<sup>2</sup>, Morocco: Foum Zguid in the Anti Atlas  $190\text{--}195$  Ma<sup>2</sup> (SCHERMERHORN et al., 1978); Liberia: Liberia-Dolerite  $180\text{--}202$  Ma<sup>2</sup> (DUPUY et al., 1988); USA and Canada: New Jersey  $194\text{--}205$  Ma<sup>2</sup>, Connecticut  $202$  Ma<sup>2</sup> and Nova Scotia  $208$  Ma<sup>2</sup> (MANSPEIZER et al., 1978); Nova Scotia  $191$  Ma (DUPUY & DOSTAL, 1984), there is good agreement of the geochemical data and the K-Ar ages. This feature seems to be a further evidence for the intimate relationship between the early Mesozoic continental tholeiite volcanism of Morocco and the initial rifting of the Atlantic Ocean.

### Conclusion

The investigated continental tholeiites have a binary chemical character. The contents of compatible elements are MORB-like, those of incompatible elements are typical for tholeiites contaminated by a crustal component (LILE enrichment, negative Nb anomaly,  $\varepsilon_{\text{Sr}}^0$  values of about +40). These quartz-normative continental tholeiites are dominated by plagioclase and pyroxene fractionation. Most of the samples have been strongly altered, characterised by K and Rb enrichment and Na, Ca and Sr depletion. The  $\varepsilon_{\text{Sr}}^0$  values increase up to +200 with enhanced alteration.  $^{87}\text{Sr}/^{86}\text{Sr}$  ratios of secondary carbonates ( $0.7083 - 0.7123$ ), which are believed to mirror the  $^{87}\text{Sr}/^{86}\text{Sr}$  ratios of the alteration fluids, argue against a submarine alteration. The determined  $^{40}\text{Ar}/^{39}\text{Ar}$  plagioclase ages range between  $196.3 \pm 1.2$  and  $210.4 \pm 2.1$  Ma, corresponding to the Norian (Rhaetian?) and Upper Sinemurian stage respectively.

### Acknowledgements

This work was part of L.F.'s Ph.D. thesis and LF is indebted to Prof. Jacobshagen for the introduction in the geology of Central Morocco. The authors thank M. Bensaid and M. Dahmani (Ministère de l'Énergie et des Mines, Rabat) for the cession of the drill core HM 2. This study was granted by the Deutsche Forschungsgemeinschaft (DFG) as a contribution to the DFG project »Mobilität aktiver Kontinentalränder« at the Berlin Free University (FUB). The authors express their gratitude to Mr. Freitag and the staff of the Forschungszentrum Geesthacht, who performed the fast neutron irradiation. We also thank two anonymous reviewers for their helpful comments and suggestions.

<sup>2</sup> recalculated with the constants recommended by STEIGER & JÄGER, 1977.



## References

- ALLÉGRE, C. J., DUPRÉ, B., RICHARD, P., ROUSSEAU, D. & BROOKS, C. (1982): Subcontinental versus suboceanic mantle, II. Nd-Sr-Pb isotopic comparison of continental tholeiites with mid-ocean ridge tholeiites, and the structure of the continental lithosphere. – *Earth Planet. Sci. Lett.*, **57**, 25–34.
- BERGER, G. W. & YORCK, D. (1981): Geothermometry from  $^{40}\text{Ar}/^{39}\text{Ar}$  dating experiments. – *Geochim. Cosmochim. Acta*, **45**, 795–811.
- BERTRAND, H., DOSTAL, J. & DUPUY, C. (1982): Geochemistry of Early Mesozoic tholeiites from Morocco. – *Earth Planet. Sci. Lett.*, **58**, 225–239.
- BROOKS, C., HART, S. R. & WENDT, I. (1972): Realistic use of two-error regression treatments as applied to rubidium-strontium data. – *Rev. of Geophys. and Space Phys.*, **2**, 551–577.
- CARTER, S. R., EVENSEN, N. M., HAMILTON, P. J. & O'NIONS, R. K. (1978): Neodymium and strontium isotope evidence for crustal contamination of continental volcanics. – *Science*, **202**, 743–747.
- COUSMINER, H. L. & MANSPEIZER, W. (1976): Triassic pollen data Moroccan High Atlas and the incipient rifting of Pangaea as Middle Carnian. – *Science*, **191**, 943–945.
- COWIE, J. W. & BASSETT, M. G. (1989): Global stratigraphic chart (1989) of the IUGS. – Supplement to *Episodes*, **12**, 2.
- DALRYMPLE, G. B. & LANPHERE, M. A. (1969): Potassium-argon dating: Principles, techniques and applications to Geochronology, 225 S., San Francisco, (Freeman).
- DUPUY, C. & DOSTAL, J. (1984): Trace element geochemistry of some continental tholeiites. – *Earth Planet. Sci. Lett.*, **67**, 61–69.
- , MARSH, J., DOSTAL, J., MICHARD, A. & TESTA, S. (1988): Asthenospheric and lithospheric sources for Mesozoic dolerites from Liberia (Africa): trace element and isotopic evidence. – *Earth Planet. Sci. Lett.*, **87**, 100–110.
- EVENSEN, N. M., HAMILTON, P. J. & O'NIONS, R. K. (1978): Rare earth abundances in chondritic meteorites. – *Geochim. Cosmochim. Acta*, **42**, 1199–1212.
- FAURE, G. (1982): The marine-strontium geochronometer. – In: Odin, G. S. (ed.), *Numerical dating in stratigraphy*, 73–79, New York, (John Wiley & Sons).
- (1986): *Principles in isotope geology*, 589 S., 2d edition, New York, (Wiley & Sons).
- FIECHTNER, L. (1990): *Geochemie und Geochronologie frühmesozoischer Tholeiite aus Zentral-Marokko*. – *Berliner geowiss. Abh.*, **118**, 76 S., Berlin.
- HAMMERSCHMIDT, K. (1986):  $^{40}\text{Ar}/^{39}\text{Ar}$  dating of young samples. – In: Hurford, A. J., Jäger, E. & Ten Cate, J. A. M. (eds.), *dating young sediments*. – *CCOP/TP*, **16**, 339–357, Bangkok.
- HAUPTMANN, M. (1990): *Untersuchungen zur Mikrofazies, Stratigraphie und Paläogeographie jurassischer Karbonatgesteine im Atlas-System Zentralmarokkos*. – unveröffentl. Dissertation, 150 S., Berlin.
- HENDERSON, P. (1984): *Rare earth element geochemistry*, 510 p., Amsterdam-Oxford-New York-Tokyo, (Elsevier).
- HERGT, J. M., CHAPPELL, B. W., FAURE, G. & MENSING, T. M. (1989): The geochemistry of Jurassic dolerites from Portal Peak, Antarctica. – *Contrib. Mineral. Petrol.*, **102**, 298–305.
- HOUTEN VAN, F. B. (1977): Triassic-Liassic deposits of Morocco and eastern North America: comparison. – *Am. Ass'n Petrol. Geol. Bull.*, **61**, 79–99.
- INGAMELLS, C. O., & ENGELS, J. C. (1977): Preparation, analysis and sampling constants for a biotite. – In: *Accuracy in trace analysis: Sampling, sample handling and analysis*. – National Bureau of Standards, Special Pub, **402**, pp 401–419.
- JACOBSHAGEN, V., GÖRLER, K. & GIESE, P. (1988): Geodynamic evolution of the Atlas System (Morocco) in post-Palaeozoic times. – In: Jacobshagen, V. (ed.), *The Atlas System of Morocco*. – Lecture Notes in Earth Sciences, 481–499, Berlin Heidelberg New York London Paris Tokyo, (Springer Verlag).
- JAQUES, A. L. & GREEN, D. H. (1980): Anhydrous melting of peridotite at 0–15 kb pressure and the genesis of tholeiitic basalts. – *Contrib. Mineral. Petrol.*, **73**, 287–310.
- KUNO, H. (1950): Petrology of Hakone volcano and the adjacent areas, Japan. – *Geol. Soc. Bull.*, **61**, 957–1020.
- LANGMUIR, CH. H., BENDER, J. F., BENICE, A. E., HANSON, G. N. & TAYLOR, S. R. (1977): Petrogenesis of basalts from the Famous Area: Mid Atlantic Ridge. – *Earth Planet. Sci. Lett.*, **36**, 133–156.
- LIU, G. J., MARUYAMA, S. & MOONSUP, C. (1987): Very low grade metamorphism of volcanic and volcanoclastic rocks – mineral assemblages and mineral facies. – In: Frey, M.: *Low temperature metamorphism*. pp 59–112. Blackie, Glasgow, London.
- LORENZ, J. (1988): Synthesis of Late Paleozoic and Triassic red-bed sedimentation in Morocco. – In: Jacobshagen, V. (ed.), *The Atlas System of Morocco*, 139–168, Berlin Heidelberg New York London Paris Tokyo, (Springer-Verlag).
- MANSPEIZER, W., PUFFER, J. H. & COUSMINER, H. L. (1978): Separation of Morocco and eastern North America: A Triassic-Liassic stratigraphic record. – *Geol. Soc. Am. Bull.*, **89**, 901–920.
- MAURER, P. (1973):  $^{40}\text{Ar}/^{39}\text{Ar}$ -Kristallisationsalter und  $^{37}\text{Ar}/^{38}\text{Ar}$ -Strahlungsalter von Apollo 11-, 12- und 17-Steinen und dem Apollo 17 »orange soil«. – Unpub. Lizentiatsarbeit, 91 S., Bern.
- MATTAUER, M., TAPPONIER, P. & PROUST, F. (1977): Sur les mécanismes de formation des chaînes intracontinentales. L'exemple des chaînes atlasiques du Maroc. – *Bull. Soc. géol. France*, (VII), **19**, 521–526, Paris.
- MATIS, A. F. (1977): Nonmarine Triassic sedimentation, Central High Atlas Mountains, Morocco. – *J. Sediment. Petrol.*, **47**, 107–119.
- MCDONALD, G. A. & KATSURA, T. (1964): Chemical composition of Hawaiian lavas. – *J. Petrol.*, **5**, 82–133.
- MCINTYRE, D. B. (1963): Precision and resolution in geochronometry. – In: Albritton, C. C. (ed.): *The fabric of geology*, 112–134, (Addison-Wesley).
- MENZIES, M. & SEYFRIED, JR., W. E. (1979): Basalt-seawater interaction: trace element and strontium isotopic variations in experimentally altered glassy basalts. – *Earth Planet. Sci. Lett.*, **44**, 463–472.
- MENZIES, M. A., LEEMAN, W. P. & HAWKESWORTH, CH. J. (1983): Isotope geochemistry of Cenozoic volcanic rocks reveals mantle heterogeneity below western USA. – *Nature*, **303**, 205–209.
- MESCHEDÉ, M. (1986): A method of discriminating between different types of mid-ocean ridge basalts and continental tholeiites with the Nb-Zr-Y diagram. – *Chem. Geology*, **56**, 207–218.
- ODIN, G. S., CURRY, D., GALE, N. H. & KENNEDY, W. J. (1982): The Phanerozoic time scale in 1981. – In: Odin, G. S. (ed.), *Numerical Dating in Stratigraphy*, **2**, 957–960, New York, (John Wiley & Sons).

- PEARCE, J. A., GORMAN, B. E. & BIRKETT, T. C. (1977): The relationship between major element chemistry and tectonic environment of basic and intermediate volcanic rocks. – *Earth Planet. Sci. Lett.*, **36**, 121–132.
- ROCHE DE LA, H., LETERRIER, J., GRANDCLAUDE, P. & MARCHAL, M. (1982): A classification of volcanic and plutonic rocks using  $R_1$   $R_2$ -Diagram and major element analyses. – Its relationship with current nomenclature – *Chem. Geology*, **29**, 183–210.
- ROEX LE, A. P. (1987): Source regions of mid-ocean ridge basalts: Evidence for enrichment processes. – In: Menzies, M. A. & Hawkesworth, C. J. (eds.), *Mantle Metasomatism*, 389–419, London, (Academic Press Harcourt Brace Jovonovich Publisher).
- SALVAN, H. M. (1974): Les séries salifères du Trias marocain: caractères généraux et possibilités d'interprétation. – *Bull. Soc. Géol. France*, **7**, 724–731.
- SCHERMERHORN, L. J. G., PRIEM, H. N. A., BOELRIJK, A. I. M., HEBEDA, E. H., VERDURMEN, E. A. TH. & VERSCHURE, R. H. (1978): Age and origin of the Messejana dolerite fault-dike system (Portugal and Spain) in the light of the opening of the north atlantic ocean. – *J. Geology*, **86**, 299–309.
- STEIGER, R. H. & JÄGER, E. (1977): Subcommittee on geochronology: convention on the use of decay constants in geo- and cosmochronology. – *Earth Planet. Sci. Lett.*, **36**, 359–362.
- STEIS, J. & WURSTER, P. (1981): Zur Strukturgeschichte des Hohen Atlas in Marokko. – *Geol. Rdsch.*, **70**, 801–811.
- STETTLER, A., EBERHARDT, P., GEISS, J., GRÖGLER, N. & MAURER, P. (1973):  $^{39}\text{Ar}$ - $^{40}\text{Ar}$  ages and  $^{37}\text{Ar}$ - $^{38}\text{Ar}$  exposure ages of lunar rocks. – *Proc. Lunar Sci. Conf.* 4<sup>th</sup>, **2**, 1865–1888.
- & ALLÉGRE, C. J. (1979):  $^{87}\text{Rb}$ - $^{87}\text{Sr}$  constrains on the genesis and evolution of the Cantal continental volcanic system (France). – *Earth Planet. Sci. Lett.*, **44**, 269–278.
- SUN, S. S. & NESBITT, W. R. (1977): Chemical heterogeneity of the archaean mantle, composition of the earth and mantle evolution. – *Earth Planet. Sci. Lett.*, **35**, 429–448.
- , NESBITT, W. R. & SHARASKIN, A. Y. (1979): Geochemical characteristics of mid-ocean ridge basalts. – *Earth Planet. Sci. Lett.*, **44**, 119–138.
- TAYLOR, S. R. & McLENNAN, S. M. (1985): *The continental crust: its composition and evolution*, 312 S., Palo Alto Oxford London Edinburgh Boston Victoria, (Blackwell Scientific Publications).
- THOMPSON, R. N., MORRISON, M. A., DICKIN, A. P. & HENDRY, G. L. (1983): Continental flood basalts ... arachnids rule OK?. – In: Hawkesworth, C. J. & Norry, M. J. (eds.), *Continental basalts and mantle xenoliths*, 158–185, Cheshire, (Shiva Publishing Limited).
- , MORRISON, M. A., HENDRY, G. L. & PARRY, S. J. (1984): An assessment of the relative roles of a crust and mantle in magma genesis: an elemental approach. – *Phil. Trans. Royal Soc. Lond.*, A **310**, 549–590.
- TURNER, G. (1971):  $^{40}\text{Ar}/^{39}\text{Ar}$  ages from the lunar maria. – *Earth Planet. Sci. Lett.*, **11**, 169–191.
- WARME, J. E. (1988): Jurassic carbonate facies of the central and eastern High Atlas rift, Morocco. – In: Jacobshagen, V. (ed.), *The Atlas System of Morocco*. – *Lecture Notes in Earth Sciences*, 481–499, Berlin Heidelberg New York London Paris Tokyo, (Springer Verlag).
- WEDEPOHL, K. H. (1988): Spilitization in the oceanic crust and seawater balances. – *Fortschr. Miner.*, **66**, 129–146.